Strange Attractors are Classified by Bounding Tori

Tsvetelin D. Tsankov and Robert Gilmore
Physics Department, Drexel University, Philadelphia, Pennsylvania 19104, USA

(Dated: August 19, 2003, *Physical Review Letters*: To be submitted.)

There is at present a doubly-discrete classification for strange attractors of low dimension, $d_L < 3$. A branched manifold describes the stretching and squeezing processes that generate the strange attractor, and a basis set of orbits describes the complete set of unstable periodic orbits in the attractor. To this we add a third discrete classification level. Strange attractors are organized by the boundary of an open set surrounding their branched manifold. The boundary is a torus with g holes that is dressed by a surface flow with $2(g-1)$ singular points. All known strange attractors in R^3 are classified by genus, g, and flow type.

Chaotic dynamics is generated by two elementary processes: stretching and squeezing. These processes are repeated over and over again in phase space. In dissipative dynamical systems this repetition builds up a strange attractor. At a topological level, strange attractors have three well-separated scales of structure. At the finest level is the fractal structure. At an intermediate level is the set of periodic orbits that provide the skeleton for the attractor. At the largest level is the global topological structure of the attractor. Roughly but accurately speaking, this is determined by the number and type of fixed points in the flow that generates the attractor. In this work we classify the global topological structure of strange attractors by certain well-defined bounding surfaces. We wish to do this because this topological classification places constraints on the global unfoldings of dynamical systems — information that is not available by local (e.g., Taylor series) methods. This new classification is important and has not previously been done.

In three dimensions there is a doubly discrete classification for strange attractors with Lyapunov exponents $\lambda_1 > 0, \lambda_2 = 0, \lambda_3 < 0$ and $d_L = 2 + \lambda_1/|\lambda_3| < 3$ [1, 2]. At a grosser level, strange attractors are classified by the branched manifolds to which they project under the Birman-Williams projection [3]. The identification

$$x \sim y \;\text{ if }\; |x(t) - y(t)| \overset{t\to\infty}{\longrightarrow} 0 \qquad (1)$$

projects the flow down along the stable manifold to a semiflow on a two dimensional surface defined by the flow and the unstable directions. The branched manifold (also known as a template or a knot-holder) describes the topological organization of all the unstable periodic orbits that exist in the strange attractor. Branched manifolds are built from two structures: splitting charts and joining charts [1–3] which describe the stretching and squeezing processes. These charts have zero- and one- dimensional singularities that prevent the branched manifold from being a manifold everywhere. Splitting and joining charts are connected in such a way that there are no free ends. Their connected union forms a compact two-dimensional structure with boundary. Branched manifolds formed in this way can be enclosed in a surface which is a torus with g holes.

Every branched manifold describes, in principle, some low dimensional strange attractor [4]. Branched manifolds have been determined for the strange attractors describing many experimental data sets [1, 2].

At a finer level a strange attractor is also classified by a basis set of orbits. These are orbits that force the existence of all the unstable periodic orbits in a chaotic flow. As control parameters are varied, many orbits supported by a branched manifold are pruned away, but those that remain are organized among themselves exactly as in the hyperbolic limit [5]. Branched manifolds are orbit organizers; basis sets of orbits provide refined descriptions of nonhyperbolic strange attractors.

Many low-dimensional strange attractors ($d_L < 3$) have been studied. All these attractors are generated by one of two types of stretch and squeeze process. One involves *only* folding, the other involves tearing (and possibly folding) [1, 2].

The stretch-fold-squeeze mechanism generates the Rössler attractor and many experimental attractors that exhibit stretching and folding according to the Smale horseshoe mechanism. These are described by a Smale horseshoe branched manifold. The Shilnikov attractor [6] is described by a subtemplate of the Smale horseshoe branched manifold. A strange attractor generated by a Nd doped fiber laser follows a reverse horseshoe mechanism. Some lasers, and sensory neurons exhibiting subthreshold oscillations, exhibit a "stretch and roll" or "gateau roulé" mechanism. The attractor for the Duffing oscillator is generated by an iterated gateau-roulé mechanism [7].

The stretch-tear-squeeze mechanism generates the Lorenz, Shimizu-Morioka, and Rikitake attractors at standard parameter values. These all share the same type of branched manifold, organized by a pair of unstable foci. More complicated attractors generated by this mechanism include dynamical systems that are n-fold

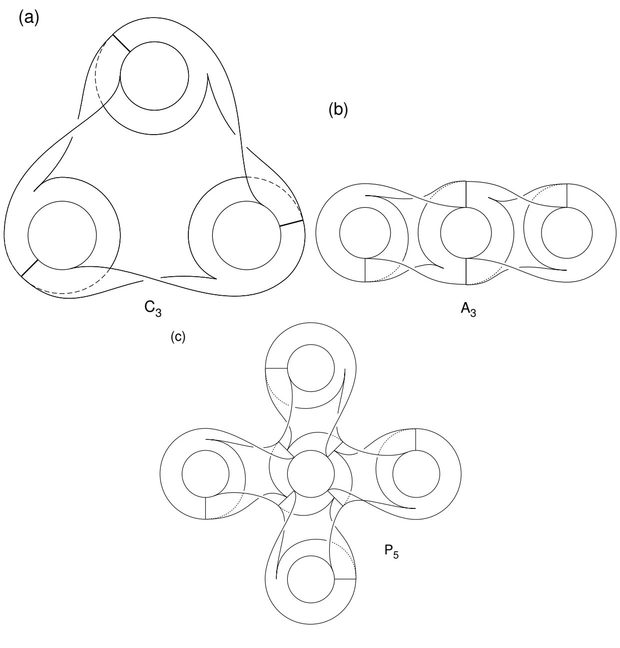

FIG. 1: Branched manifolds describing different stretch-tear-squeeze mechanisms. (a) 3-fold cover of the Rossler system with C_3 symmetry. (b) 2-fold cover and (c) 4-fold cover of the Lorenz system with rotation symmetry about an axis through a focus.

covers of the Rössler attractor with rotational symmetry. Some of these are organized by n symmetrically placed unstable foci, and are generalizations of the 3-fold cover whose branched manifold is shown in Fig. 1(a) [8, 9]. Another class of strange attractor is obtained from the Lorenz equations by constructing the double cover with 2-fold symmetry with respect to rotations about one of the foci, as shown in Fig. 1(b). The cover of the Lorenz attractor with two-fold rotation symmetry about an axis passing through the saddle is topologically similar to a cover of the Rössler attractor with four-fold symmetry about a rotation axis. The branched manifold for a four-fold cover of the Lorenz system with rotation axis passing through one of the foci is shown in Fig. 1(c) [9].

We seek to construct a mechanism for organizing branched manifolds, in analogy with the way branched manifolds organize periodic orbits in a strange attractor. The organizing structures are the surfaces of tori with g holes. These genus-g surfaces bound regions of phase space in which a flow surrounds the semiflow on the branched manifold [1, 2]. We argue below that such surfaces, dressed with a canonical, compatible flow, classify branched manifolds and describe their possible perestroikas in the same way that branched manifolds organize periodic orbits in a strange attractor and describe their possible unfoldings.

The key to the classification that is described below is the robust presence of "holes." It is necessary to get rid of structurally unstable holes in the attractor or its branched manifold. Such holes can be created by three mechanisms:

1. Holes are normally placed between branches in a branched manifold that is created by a folding mechanism (c.f., [1]). This is done to emphasize that they represent a hyperbolic limit. This limit is never seen either in experimental data nor in flow simulations.

2. Holes are created when the flow is restricted to a subtemplate of a larger, fully expanding template. This is seen in the Shilnikov [6] attractor and in the Shimizu-Morioka attractor [1, 10] as parameter values are varied. We exclude these holes by assuming the allowed grammar has no forbidden symbol sequences [11].

3. Holes can be generated by embedding short experimental data sets, particularly when one or more of the branches describes very unstable orbit segments (c.f., [2]).

Once structurally unstable holes have been removed, we proceed as follows. The flow in the strange attractor is projected down to a semiflow on the branched manifold using (1). There are no fixed points on the branched manifold. The branched manifold is "fattened up" to a 3-dimensional manifold by means of short intervals of length ϵ passing transversely through each point of the branched manifold. The flow in this thin three dimensional space limits to the semiflow on the branched manifold and has Lyapunov exponents $\lambda_1 > 0$, $\lambda_2 = 0$, and $\lambda_3 < 0$ with $d_L = 2 + \lambda_1/|\lambda_3| < 3$.

The boundary of this three-dimensional space is a trapping surface. Once the flow passes through the boundary it relaxes exponentially to the branched manifold. The boundary is a closed orientable two dimensional manifold. All such surfaces have been classified by their genus, $g \geq 0$. For $g = 0$ the surface is the sphere S^2. For $g = 1$ the surface is the simple torus. For $g \geq 2$ the surface is the torus with g holes, also known as a sphere with g handles [2, 12].

On the surface the flow has a normal component and a tangential component. The tangential component of the flow may have singularities. Singularities occur where the flow is perpendicular to the boundary. At such points the singularity is of saddle type, since there is one unstable direction (the λ_1 direction) and one stable direction (λ_3). The index of each singularity is $(-1)^{n_u} = -1$, where $n_u = 1$ is the number of unstable directions at the singular point.

The Euler characteristic $\chi(\mathcal{S})$ relates the topology of a surface $\mathcal{S}$ with the properties of any vector field defined on that surface. For a genus-g surface, the Euler characteristic is χ(genus-g)$= 2 - 2g$. Since all singularities of the projected flow have index -1, there are exactly $2g-2$ singularities of the flow restricted to the genus-g surface.

As a final step, we dress the genus-g surface surrounding a branched manifold with a flow in canonical form.

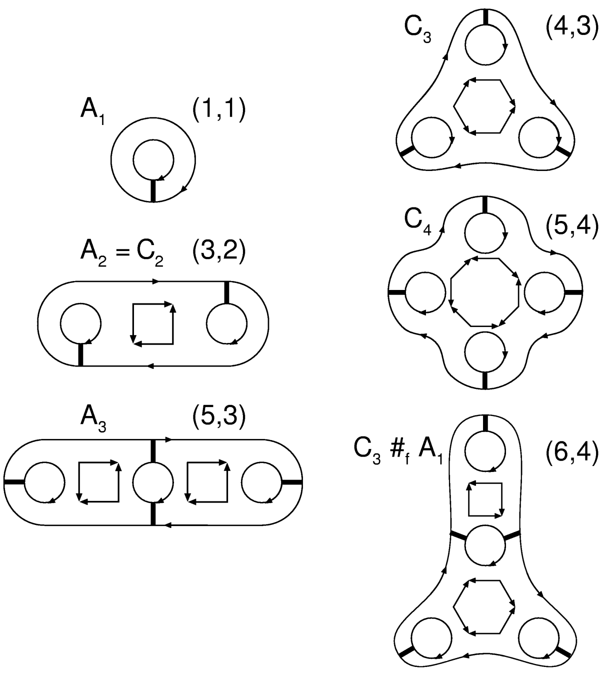

FIG. 2: Canonical dressed tori with genus $g \leq 6$. For each canonical form we provide a name and the index pair (g, n).

This canonical form is easy to describe. The torus with g holes is projected onto a 2-dimensional planar surface in such a way that the projection is a disk with g interior holes. All singularities are on the boundaries of the holes. The outer boundary of the disk has no singularities, and on this boundary the flow is in a single direction. Some (n) of the interior holes have no singularities: on these holes the flow is in the same direction as on the outer boundary. All $2g - 2$ singularities occur on the remaining interior holes: all such holes have an even number of singularities, starting with a minimum number of four singularities.

In Fig. 2 we show canonical forms for flows with genus $g \leq 6$. We identify each by name and index pair (g, n). Strange attractors generated by a stretch-fold-squeeze mechanism can all be embedded in a solid torus with one hole. The van der Pol attractor can also be embedded in a torus with one hole. However, a cross section of the attractor exhibits an annular structure, so that this attractor has both an exterior and an interior boundary: a torus within a torus. The Lorenz, Shimizu-Morioka, and Rikitake attractors can be enclosed in surfaces with genus 3.

There are two simple series of canonically dressed surfaces of genus g. There are chains A_n $(n \geq 1)$ with n interior holes on which the flow is unidirectional and $n - 1$ separating holes with four singularities each. The genus is $g = 2n - 1$. A_1, A_2 and A_3 are shown in Fig. 2. There are cycles C_n $(n \geq 2)$ having n holes on which the flow is unidirectional, and one interior hole with $2n$ singularities. The genus is $g = n + 1$. C_2, C_3 and C_4 are shown in Fig. 2. For these series $A_2 = C_2$ but $A_n \neq C_n$. All other canonically dressed forms can be obtained from these two simple series by a simple process $(\#_f)$ based on forming the connected sum $(\#)$ [2, 12] of two tori. The tori are connected using the process $\#$ and this larger torus is dressed with a flow having canonical form. The torus $C_3 \#_f A_1$ is shown in Fig. 2.

In Table I we classify all known strange attractors that have been studied in R^3 according to their genus and type. All attractors generated by the stretch-fold-squeeze mechanism are enclosed by boundaries of type A_1. The van der Pol attractor has both an interior and an interior boundary: it is contained in $A_1 \cup A_1$. The Lorenz, Shimizu-Morioka, and Rikitake attactors are enclosed by $A_2 = C_2$. There is a class of covers of the Rössler dynamical system that is invariant under the rotation group C_n generated by rotations about the z axis through $2\pi/n$ radians [8, 9]. These attractors are enclosed by C_n. Several different types of attractors can be generated by covers of the Lorenz system with n-fold rotation symmetry, depending on where the rotation axis is placed [9]. If it passes through the saddle, the cover is enclosed by a surface of type C_{2n}. If the axis passes through a focus, the cover is contained in a "pinwheel" P_{n+1} (P_5 is shown in Fig. 1(c)). Multispiral attractors with n spirals are contained in A_n [13].

TABLE I: All known strange attractors of dimension $d_L < 3$ are bounded by one of the standard dressed tori.

Strange Attractor	Dressed Torus
Rossler, Duffing, Burke and Shaw	A_1
Various Lasers, Gateau Roule	A_1
Neuron with Subthreshold Oscillations	A_1
Shaw-van der Pol	$A_1 \cup A_1$
Lorenz, Shimizu-Morioka, Rikitake	A_2
Multispiral attractors	A_n
$\mathcal{C}_n$ Covers of Rossler	C_n
$\mathcal{C}_2$ Cover of Lorenz$^{(a)}$	C_4
$\mathcal{C}_2$ Cover of Lorenz$^{(b)}$	A_3
$\mathcal{C}_n$ Cover of Lorenz$^{(a)}$	C_{2n}
$\mathcal{C}_n$ Cover of Lorenz$^{(b)}$	P_{n+1}
$2 \rightarrow 1$ Image of Fig. 8 Branched Manifold	A_3
Fig. 8 Branched Manifold	P_5

$^{(a)}$ Rotation axis through origin.
$^{(b)}$ Rotation axis through one focus.

Poincaré sections exist for all these canonical forms. For A_1 it is a disk. This is represented by a single line connecting the interior circle with the boundary circle for A_1 in Fig. 2. For the genus-g case $(g > 1)$ the Poincaré section is the union of $g - 1$ disks. These all connect one of the n interior circles without singularities to the exterior boundary. The Poincaré sections for the flows in $A_2, A_3, C_3, C_4, C_3 \#_f A_1$ are unions of $2, 4, 3, 4, 5$ disks, respectively. The locations of these components are indicated in Fig. 2. Transition matrices for the branches of branched manifolds bounded by a genus-g surface must be compatible with transition matrices for the components of its Poincaré section. For example, the branched manifold of the Rössler attractor has two branches labeled 0, 1 and its three-fold cover, enclosed by C_3, has branch lines A, B, C. The branched manifold has six branches $A0, A1, B0, B1, C0, C1$. The transition matrices for the components of the Poincaré section and the branched manifold are

$$\begin{array}{c} A \\ B \\ C \end{array} \begin{bmatrix} 1 & 1 & 0 \\ 0 & 1 & 1 \\ 1 & 0 & 1 \end{bmatrix} \qquad \begin{array}{c} A0 \\ A1 \\ B0 \\ B1 \\ C0 \\ C1 \end{array} \begin{bmatrix} 1 & 1 & 0 & 0 & 0 & 0 \\ 0 & 0 & 1 & 1 & 0 & 0 \\ 0 & 0 & 1 & 1 & 0 & 0 \\ 0 & 0 & 0 & 0 & 1 & 1 \\ 0 & 0 & 0 & 0 & 1 & 1 \\ 1 & 1 & 0 & 0 & 0 & 0 \end{bmatrix}$$

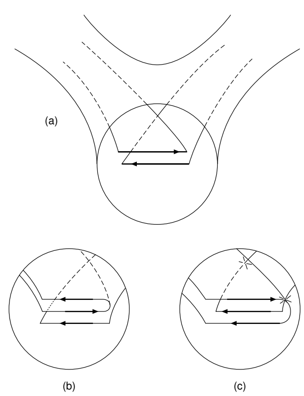

FIG. 3: Constraints on global perestroikas. (a) Two branches through different parts of a genus-g torus merge near a branch line. As control parameters vary, one of the branches may fold. (b) Some folding configurations are allowed, (c) while others violate causality.

Bounding tori provide constraints on the perestroikas that can take place as control parameters are varied. Fig. 3 provides an illustration. Fig. 3(a) shows two branches approaching a branch line. The two branches come through distinct flow tubes in the genus-g torus. As control parameters or experimental conditions change, the branches may grow and fold. Some folding directions are compatible with the geometry (Fig. 3(b)), while others are not (Fig. 3(c)). The flow in Fig. 3(c) violates causality. In this way the geometry of the genus-g boundary and the existence and uniqueness theorem for flows place constraints on the global perestroikas for dynamical systems. In this sense genus-g surfaces are branched manifold organizers in much the same way that knot holders are periodic orbit organizers.

Most of the attractors studied so far do not have the complexity of A_n or C_n, $n > 2$. The reason is as follows. Attractors generated by complicated tearing mechanisms possess many fixed points. They are generated by flows around more than two unstable fixed points of focus type. However, almost all attractors that have been studied are obtained by polynomial truncation of the forcing terms in the equations $dx_i/dt = f_i(x_1, x_2, x_3)$. Polynomial truncations tend to be low order: most are of the second or third degree. There is a theorem from algebraic topology (Bezout's theorem) that relates the number of fixed points to the polynomial structure of the forcing terms. In essence, low order truncations are not compatible with the large number of fixed points in flows that generate strange attracctors with genus g, $g > 3$. To be precise, covers of the Rössler and Lorenz systems that provide attractors of type A_n or C_n, $n > 2$, do not have polynomial forcing terms and therefore fall outside the scope of most modeling efforts. Exceptions involve piecewise linear functions [13].

This work is partially supported by NSF Grant PHY 9987468.

REFERENCES

[1] R. Gilmore, Revs. Mod. Phys. **70**(4), 1455 (1998).
[2] R. Gilmore and M. Lefranc, *The Topology of Chaos*, NY: Wiley, 2002.
[3] J. Birman and R. F. Williams, Cont. Math. **20**, 1 (1983).
[4] G. B. Mindlin, X.-J. Hou, H. G. Solari, R. Gilmore, and N. B. Tufillaro, Phys. Revl Lett. **64**, 2350 (1990).
[5] F. Papoff, A. Fioretti, E. Arimondo, G. B. Mindlin, H. G. Solari, and R. Gilmore, Phys. Rev. Lett. **68**, 1128 (1992).
[6] C. Letellier, P. Dutertre, and B. Maheu, Chaos **5**, 271 (1995).
[7] R. Gilmore and J. W. L. McCallum, Phys. Rev. E**51**, 935 (1995).
[8] R. Miranda & E. Stone, Physics Letters A, **178**, 105-113, 1993.
[9] C. Letellier & R. Gilmore, Physical Review E, (in press).
[10] A. L. Shil'nikov, Physica D**62**, 338 (1993).
[11] D. Auerbach and I. Procaccia, Phys. Rev. A**41**, 6602 (1990).
[12] Jeffrey R. Weeks, *The Shape of Space* (Second Edition), NY: Marcel Dekker, 2002.
[13] M. A. Aziz-Alaoui, Int. J. Bifurcation and Chaos **9**(6), 1009 (1999).